# Structure and Phase Transitions of Ethyl 4′-n-undecyloxybiphenyl-4-carboxylate and Its Acid Derivative

Delia López-Velázquez [a] , Armando R. Hernández-Sosa [a] , Sylvain Bernès [b] , Ernesto Pérez [c] & Juan P. Fernández-Blázquez [c]

[a] Facultad de Ciencias Químicas, BUAP, Ciudad Universitaria, Puebla, México

[b] DEP, Facultad de Ciencias Químicas, UANL, Monterrey, N.L., México

[c] Instituto de Ciencia y Tecnología de Polímeros, CSIC, Madrid, Spain

Version of record first published: 05 Apr 2011

PLEASE SCROLL DOWN FOR ARTICLE

Taylor & Francis
Taylor & Francis Group

# Structure and Phase Transitions of Ethyl 4′-*n*-undecyloxybiphenyl-4-carboxylate and Its Acid Derivative

## Delia López-Velázquez[1], Armando R. Hernández-Sosa[1], Sylvain Bernès[2], Ernesto Pérez[3], and Juan P. Fernández-Blázquez[3]

[1]Facultad de Ciencias Químicas, BUAP, Ciudad Universitaria, Puebla, México
[2]DEP, Facultad de Ciencias Químicas, UANL, Monterrey, N.L., México
[3]Instituto de Ciencia y Tecnología de Polímeros, CSIC, Madrid, Spain

*Ethyl 4′-n-undecyloxybiphenyl-4-carboxylate,* **2(11)OBC***, and 4′-n-undecyloxybiphenyl-4-carboxylic acid,* **(11)OBC***, are smectic liquid crystals precursors of low molecular weight premesogens, and of potential liquid crystal macromolecules. The single-crystal X-ray study of* **2(11)OBC** *showed that it crystallizes in a non-centrosymmetric space group with molecules stacked along the short axis [010] and [001] without significant π···π or CH···π interactions. Such an arrangement may explain its strong tendency to form smectic mesophases. Both biphenyl derivatives have a rich polymesomorphism whose phase sequences were determined by DSC, optical microscopy and diffraction profiles using synchrotron radiation. These profiles indicated quite similar phase transitions in the two samples, although very different transition temperatures. Thus, the phase transitions (on cooling) of* **2(11)OBC** *are: Isotropic → SmA (101°C) → SmB (88°C) → SE (79°C) → crystal phase (43°C), while those (on cooling) of* **(11)OBC** *are the following: Isotropic → SmA (246°C) → SmB (192°C) → SX (162°C) → SE (148°C) → crystal phase (62°C). The much higher transition temperatures for the acid derivative are explained by considering that this molecule forms dimers through classical O–H···O hydrogen bonds involving the carboxylic groups.*

## INTRODUCTION

Biphenyl derivatives have been extensively studied because of their application in liquid crystal displays [1]. Furthermore, biphenyl esters and their acids are able to undergo functionalization reactions, providing access to a variety of compounds [2]. On the other hand, liquid crystalline polymers with mesogenic side chains (SCLCPs) have attracted special interest because of the possible applications in the fields of non-linear optics, optical storage and electro-optic displays [3]. SCLCPs can be obtained either by chemical modification of a pre-polymer with a functionalized liquid crystal or by polymerization of a liquid crystal monomer.

Gray *et al.* [4] synthesized and studied the mesomorphic behavior of some 4′-*n*-alkoxybiphenyl-4-carboxylates [structure (***m***)**OBC** in Scheme 1], and their ester derivatives *n*-alkyl-4′-*n*-alkoxybiphenyl-4-carboxylates, ***n(m)*OBC** (Scheme 1) where ***n*** = 1–3 is the number of C atoms of the aliphatic alcohol derivative, and ***m*** = 1–10, 12, 16, 18 is the number of C atoms in the alkyl tail. However, they did not synthesize **(11)OBC**, neither the derived ester **2(11)OBC**, which will be described in this paper. They reported that the acids with ***m*** = 1–4 are not mesomorphic, while the acids with ***m*** = 5–10 develop smectic-nematic mesophases, and those with ***m*** = 12, 16 and 18 develop only smectic phases. In the case of their ethyl esters **2(*m*)OBC** they described that the first four members with ***m*** = 1–4 are non-mesomorphic, while the other nine ethyl esters, corresponding to ***m*** = 5–10, 12, 16 and 18, develop only smectic phases. In their work
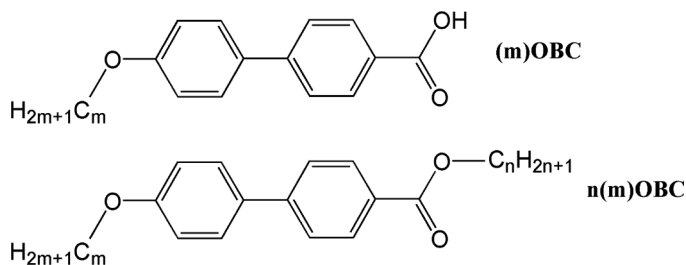


**SCHEME 1** General formula of 4′-*n*-alkoxybiphenyl-4-carboxylates and *n*-alkyl-4′-*n*-alkoxybiphenyl-4-carboxylates.

        *D. López-Velázquez et al.*

$(CH_2)_i$ —$CH(Me)$ —$O$—$(CO)_q$ —$C_nH_{2n+1}$

$(X)_p$

$H_{2m+1}C_m$
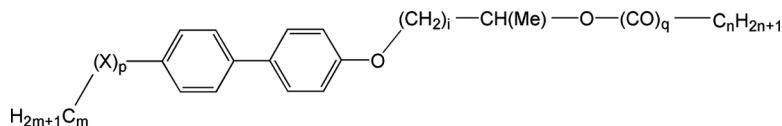
**SCHEME 2** Optically active biphenyl derivatives [5], where $X = O$, $CO$ or $OCO$; $p$, $q = 0$ or $1$ and $i = 1$–$6$; $\boldsymbol{m} = 3$–$20$; $\boldsymbol{n} = 1$–$20$ (optionally substituted).

they did not report DSC or X-ray analysis for none of the acids and corresponding ethyl esters. Therefore, the accurate types of meso-phases were not described.

It should be also mentioned that Isoo and coworkers [5] reported isomers of **(11)OBC** ($C_{24}H_{32}O_3$), and its ethyl ester **2(11)OBC** ($C_{26}H_{36}O_3$). However, these isomers belong to a family of chiral esters whose general formula is given in Scheme 2.

Therefore, the importance of ethyl 4′-*n*-undecyloxybiphenyl-4-carboxylate and its acid stems from their ability to potentially undergo functionalization reactions, providing access to a variety of compounds.

We report here the analysis by DSC, optical microscopy and synchrotron X-ray diffraction of the phase transitions for **(11)OBC** and **2(11)OBC**. Moreover, with the aim of gaining insight in the pack-ing patterns of the **2(11)OBC** mesogenic arrangement, its room-temperature structure was also determined by single crystal X-ray analysis. Such a solid-state structural analysis was unfortunately not achieved for **(11)OBC**, due to the poor solubility of this acid, avoiding growth of suitable single crystals.

## EXPERIMENTAL

Ethyl-4′-hydroxy-4-biphenylcarboxylate (98%), chloroform-d (99.9%), (methyl sulfoxide)-d$_6$ (99.9%) and 1-bromo-undecane (99%) were purchased from Sigma-Aldrich and were used as received. Dimethyl-formamide (DMF) was purified according to a standard procedure. Other chemicals were of reagent grade and used without further purification. The chemical structures of all the materials prepared, intermediates and final products, were analyzed by a combination of nuclear magnetic resonance spectroscopy (NMR), infrared spec-troscopy (FTIR) and C, H elemental analysis. Analytical data were found to be fully consistent with the assigned structures.

^{1}H-NMR and ^{13}C-NMR spectra were acquired with a Varian (400 MHz) spectrometer. The NMR samples were prepared as 10–20% (w/v) solutions in CDCl$_3$ or DMSO-$d_6$. Spectra were usually recorded at room temperature.

FTIR analyses were performed on a Perkin–Elmer Spectrum One spectrometer. The samples were prepared by dissolving the material in a volatile solvent, placing a few drops of the solution on a diamond cell, and then allowing the solvent to evaporate.

Diffraction data for **2(11)OBC** were collected at 23°C on a Bruker P4 diffractometer, using standard procedures [6] and the structure solved and refined using the *SHELX97* package [7]. Measured Friedel pairs were merged in the final least-squares cycles, since no significant anomalous scattering effects are produced by this organic crystal. Bond length C16–C17 was restrained to 1.53(1) Å, otherwise an unreasonably short bond length was obtained at convergence, probably because of an unresolved disorder. All H atoms were placed in calculated positions and refined isotropically using a riding model approximation. Further details and complete geometric data may be obtained from the archived CIF, and raw diffraction data are available on request.

The thermal behavior of **2(11)OBC** and **(11)OBC** was studied by thermogravimetric analysis (TGA) and differential scanning calorimetry (DSC). Subsequently, the nature of the phases involved was analyzed by optical microscopy and by real-time diffraction experiments.

Decomposition temperatures were determined in nitrogen atmosphere by thermogravimetric analysis using a TGA Q50 (TA Instruments, New Castle, DE). A Perkin–Elmer DSC7 Calorimeter equipped with an auto-cool accessory and Thermal Analysis Data Station was employed for DSC studies. The scans were carried out under a nitrogen atmosphere. Transition temperatures were collected during heating and cooling scans, at different rates: 20°C/min for **(11)OBC** and 8°C/min for **2(11)OBC**, and for several cycles.

A Carl-Zeiss Amplival D microscope, in conjunction with a Linkam TMS92 hot stage with its control unit, was used for the polarized optical microscopy (POM) experiments. This microscope was also equipped with a video camera.

Real-time variable-temperature X-ray scattering experiments were performed using synchrotron radiation ($\lambda = 0.150$ nm) in the soft-condensed matter beam-line A2 at HASYLAB (Hamburg, Germany). A MAR-CCD detector placed at a distance of 169 mm from the sample was used, covering the spacings interval from around 10 to 0.3 nm (wide, WAXS, and middle-angle scattering, MAXS, regions). The detector calibration for spacings was made with a sample of silver behenate ($AgC_{22}H_{43}O_2$), which gives a well-defined diffraction at a spacing of 5.838 nm, and several other orders spacings.
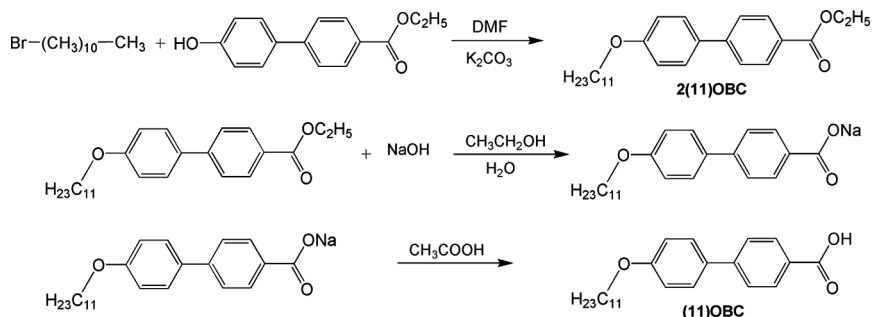
**SCHEME 3** Synthesis of **2(11)OBC** and **(11)OBC**.

## Synthesis and Characterization of 2(11)OBC, C$_{26}$H$_{36}$O$_3$

Ethyl-4$'$-$n$-undecyloxybiphenyl-4-carboxylate was synthesized follow-ing a procedure reported in the literature [8]. Basically, this compound was obtained by reacting ethyl 4$'$-hydroxy-4-biphenylcarboxylate and 1-bromo-$n$-undecane in DMF at 100°C for 24 h (see Scheme 3). 90% yield. IR (ATR) 2917, 1714, 1602, 1284, 816 cm$^{-1}$. $^1$H-NMR (CDCl$_3$)$\delta$: 0.88 (t, 3H), 1.47 (m, 2H), 1.27 (m, 7H), 1.80 (m, 2H), 3.99 (m, 2H), 6.99 (m, 2H), 7.54 (d, 2H), 7.62 (d, 2H), 8.06 (d, 2H), 4.38 (d, 2H), 1.40 (t, 3H). $^{13}$C-NMR (CDCl$_3$) $\delta$: 166.62, 159.44, 145.19, 132.21, 130.05, 128.53, 128.31, 126.39, 114.93, 68.15, 60.88, 31.92, 29.62, 29.41, 29.26, 26.06, 22.70, 14.38, 14.12. Anal. Calcd for C$_{26}$H$_{36}$O$_3$: C 78.75, H 9.15. Found: C 78.88, H 9.18. Colorless single crystal, $0.60 \times 0.60 \times 0.14$ mm$^3$; monoclinic, $Cc$; $a = 50.369(8)$, $b = 7.5607(13)$, $c = 6.1879(18)$ Å, $\beta = 92.976(17)$°; radiation: Mo-$K\alpha$ ($\lambda = 0.71073$ Å), $\theta_{\max} = 27.5$°; 2685 unique data for 263 refined parameters; $R_1$ [$I > 2\sigma(I)$] $= 0.0579$, $wR_2$ [all data] $= 0.1805$.

## Synthesis and Characterization of (11)OBC, C$_{24}$H$_{32}$O$_3$

4$'$-$n$-Undecyloxybiphenyl-4-carboxylic acid was obtained by a classic saponification of its ester with sodium hydroxide, as described in Scheme 3. The sodium salt was acidified with acetic acid under reflux (104°C) for 25 min. After dissolution, the mixture was then allowed to cool to room-temperature, and subsequently cooled to 0°C. A micro-crystalline powder which formed was collected by filtration, washed with large amounts of water, and dried under vacuum at 45°C, to yield 93% of white powder. IR (ATR) 3300–2500, 2917, 1685, 1603, 1290, 836 cm$^{-1}$. $^1$H-NMR (DMSO-$d_6$, 70°C) $\delta$: 0.85 (t, 3H); 1.42 (m, 2H); 1.25 (m, 14H); 1.72 (m, 2H); 4.01 (t, 2H); 7.02 (d, 2H); 7.63 (d, 2H);

7.72 (d, 2H); 7.97 (d, 2H). $^{13}$C-NMR (DMSO-$d_6$, 70°C) $\delta$: 167.75, 159.80, 144.73, 131.99, 130.55, 129.71, 128.71, 126.69, 115.84, 68.48, 31.91, 29.59, 29.38, 29.29, 26.14, 22.67, 14.44. Anal. Calcd for $C_{24}H_{32}O_3$: C, 78.22; H, 8.75. Found: C, 78.27; H, 8.79.

## RESULTS AND DISCUSSION

### Crystal Structure of 2(11)OBC

As expected, **2(11)OBC** crystallizes in a strongly anisotropic unit-cell, with a long/short parameters ratio $a/c > 8$. The molecule is built-up on a biphenyl core *para*-substituted by the ethyl ester and *n*-undecyloxy functional groups (Fig. 1, inset). The latter presents an all-*trans* conformation, as found in the closely related derivative 4-cyano-4′-(*n*-undecyloxy)biphenyl [9]. In **2(11)OBC**, the dihedral angle between aromatic rings is 12.7(2)°, significantly smaller than that found in the cyano derivative (31.4°). However, this conformation is consistent with other *para*-substituted biphenyl derivatives, for which dihedral angles fall in the range 0 to 60°. Such conformational variations are generally believed to be a consequence of crystal packing effects rather than steric or electronic effects.

Rajnikant *et al.* structurally characterized a number of 4-cyano-4′-(*n*-alkyloxy)-biphenyl derivatives, namely with $m = 8$ [10], $m = 10$ [11], $m = 11$ [9], and $m = 12$ [11] alkyl chains. The case $m = 8$, *i.e.*, 4-cyano-4′-octoxybiphenyl, is of particular interest, since a transition
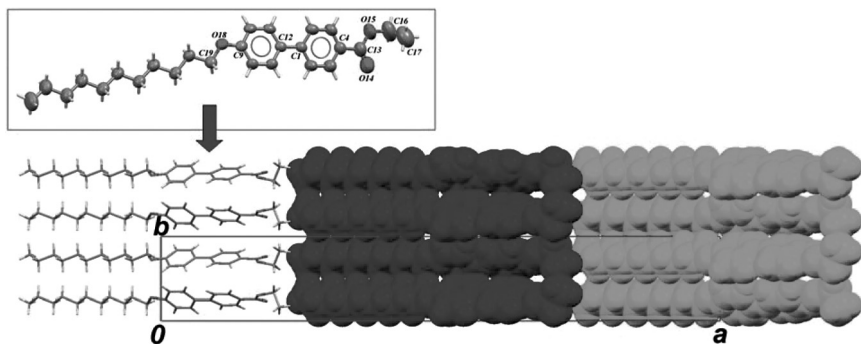


**FIGURE 1** Crystal structure of **2(11)OBC** viewed along [001]. Left molecules are in a stick style while right molecules are shown in a spacefill style, in order to appreciate how molecules stack along [010]. Colors for spacefill molecules are arbitrary. The inset represents an ORTEP-like plot of **2(11)OBC**, with displacement ellipsoids for non-H atoms at the 50% probability level.

to smectic phase has been detected at 54.5°C [10]. Moreover, polymorphic phases have been reported for this molecule [12,13]. As a common feature, all these molecules crystallize in centrosymmetric space groups. In contrast, **2(11)OBC** crystallizes in a non-centrosymmetric space group, *Cc*, allowing a different arrangement for molecules in the crystal, which, in turn, should facilitate the polymesomorphism observed for this biphenyl (see *infra*). Molecules are stacked along the short [010] and [001] axis (Fig. 1) with aliphatic chains placed parallel within a stack. These stacks are repeated through translational symmetry operators, including *C* cell centering. No significant $\pi\cdots\pi$ or CH$\cdots\pi$ intermolecular interactions are present in the crystal structure, a feature obviously related to the low melting point of **2(11)OBC**.

For the acid **(11)OBC**, attempts to obtain single crystals were unsuccessful, its solubility being low and limited to some polar aprotic solvents, like acetone, DMF and DMSO. IR spectrum for this compound displays a broad O–H stretch vibration (3300–2500 cm$^{-1}$), indicative of intermolecular hydrogen bonding, and a strong sharp band at 1685 cm$^{-1}$ associated to H-bonded carbonyl stretching. These bands are characteristic of centrosymmetric dimers formed through strong O–H$\cdots$O hydrogen bonds involving carboxylic functionalities [14,15], and may explain both the high melting point and the low solubility [16] observed for this compound.

## Thermal Behavior of 2(11)OBC and (11)OBC

The TGA of **(11)OBC** showed a good thermal stability up to 250°C and a single-step weight loss with maximum loss rate at 366°C (Fig. 2). The temperature for 9.91% weight loss was 284.2°C. The DSC curves of **(11)OBC** are shown in Figure 3 for the first melting and subsequent cooling. Several transitions are found in both curves. Thus, the melting curve shows four endothermic peaks (one of them of very small intensity) centered at 115.8, 172.2, 200.5 and 254.2°C, with enthalpies of 63.3, 45.3, 2.0 and 56.0 J/g, respectively. The thermal transition data for **(11)OBC**, compared to those of its ethyl ester, are given in Tables 1 and 2. The phases involved in the different transitions will be analyzed in the section devoted to synchrotron diffraction data.

The DSC curves corresponding to **2(11)OBC** are shown in Figure 4. Four transitions can be observed. Thus, the cooling curve shows four exothermic peaks, three of them very sharp (at 100.9, 87.6 and 78.7°C) and a low-temperature one much broader, centered at 43.4°C and with the onset at *ca*. 50°C. The thermodynamic data for both the melting and cooling runs are presented in Tables 1 and 2, respectively, and can be compared to those computed for **(11)OBC**. It can
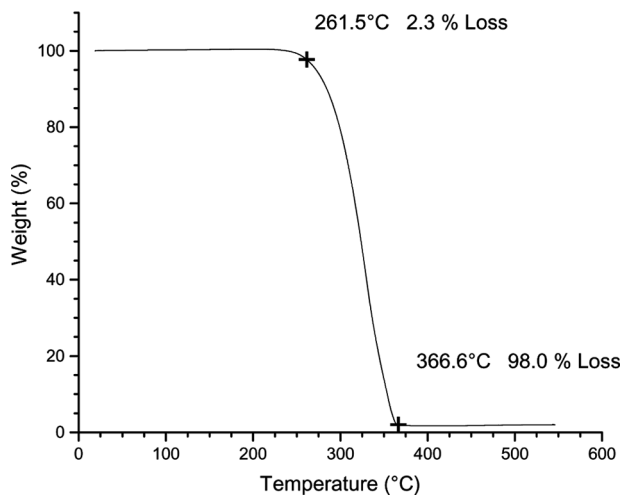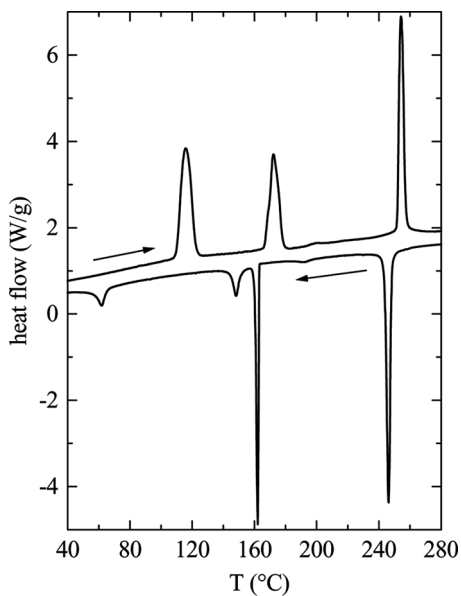
**FIGURE 2** Thermogravimetric curve of **(11)OBC**.



**FIGURE 3** DSC curves of the biphenyl derivative **(11)OBC** corresponding to the first melting and the subsequent cooling.

*D. López-Velázquez et al.*

**TABLE 1** Thermal Properties and Phase Transitions Involved for **2(11)OBC** and **(11)OBC** in the First DSC Heating Run

| Sample | $T$,°C ($\Delta H$, J/g) | $T$,°C ($\Delta H$, J/g) | $T$,°C ($\Delta H$, J/g) | $T$,°C ($\Delta H$, J/g) |
|---|---|---|---|---|
| **2(11)OBC** | **SE** 79.0 (90.8) | **SmB** 81.8 (3.0) | **SmA** 90.0 (7.0) | **I** 104.0 (25.5) |
| **(11)OBC** | **SE** 115.8 (63.3) | **SX + SmB** 172.2 (45.3) | **SmA** 200.5 (2.0) | **I** 254.2 (56.0) |

I = isotropic, SmA = Smectic A, SmB = Smectic B, SE = Smectic crystal E, SX = unknown smectic crystal.

be observed that the transition temperatures are much higher in the case of the acid, **(11)OBC**, a feature consistent with IR data and the assumed dimeric structure in the solid state.

All these phase transitions are reversible and do not change on repeated heating and cooling cycles. It should be pointed out that, in the case of the acid, the onset decomposition temperature is reached above 255°C (see Fig. 2).

## Optical Textures of (11)OBC and 2(11)OBC

When **(11)OBC** is cooled from the isotropic phase, the first birefringent texture is observed at *ca*. 240°C (Fig. 5a). On decreasing of the temperature, that texture coexists with a granulated one (Fig. 5b, $T = 230$°C). Considering that the first transition observed in the DSC experiment (Fig. 3) has a low enthalpy and very low undercooling, the first phase formed from the isotropic melt may be assumed to be a low-ordered smectic mesophase. During the two following DSC transitions (exotherms at 162.1 and 148.3°C) the texture changes to a mosaic texture (Fig. 5c, $T = 135$°C), and it is not possible to distinguish optical changes between both DSC transitions. This texture is typical of mesophases with higher order [17,18]. On further cooling, several lines appear superimposed on the mosaic structure (Fig. 5d,

**TABLE 2** Thermal Properties and Phase Transitions Involved for **2(11)OBC** and **(11)OBC** in the DSC Cooling from the Isotropic Melt

| Sample | $T$,°C ($\Delta H$, J/g) | $T$,°C ($\Delta H$, J/g) | $T$,°C ($\Delta H$, J/g) | $T$,°C ($\Delta H$, J/g) |
|---|---|---|---|---|
| **2(11)OBC** | **SmA** 100.9 (24.8) | **SmB** 87.6 (6.7) | **SE** 78.7 (5.6) | **K** 43.4 (57.8) |
| **(11)OBC** | **SmA** 246.3 (56.4) | **SmB** 191.6 (2.1) | **SX** 162.1 (32.1) **SE** 148.3 (12.3) | **K** 61.9 (12.6) |

SmA = Smectic A, SmB = Smectic B, SE = Smectic crystal E, SX = unknown smectic crystal, K = crystal.
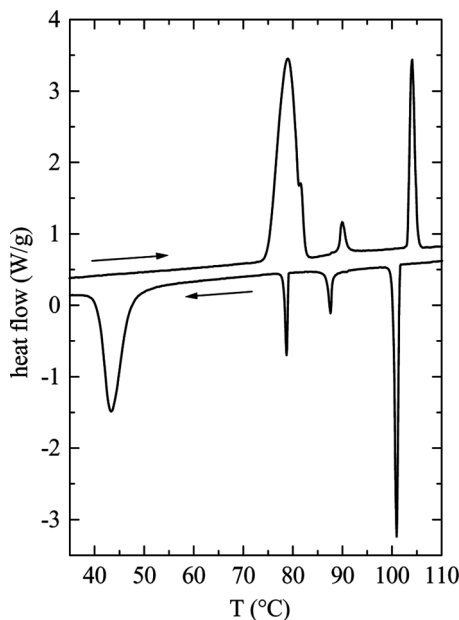
**FIGURE 4** DSC curves of the biphenyl derivative **2(11)OBC** corresponding to the first melting and the subsequent cooling.

$T = 60°C$), corresponding to the last exothermic peak at 61.9°C. Most probably, an ordered crystal structure has then been reached.

In the case of **2(11)OBC**, the representative textures observed during the cooling from the isotropic melt are shown in Figure 6. A fan-shaped texture is first observed at 103°C (Fig. 6a). This texture, typical of a low ordered mesophase [17–19], does not present important changes when cooling down to 85°C, although variations in the light intensity can be observed (Fig. 6b). At 75°C, concentric arcs appear in the fan-shaped texture (Fig. 6c). This texture [17] is characteristic of highly ordered smectic crystals, as for SE phases. Finally, a granulated texture is obtained at lower temperatures (Fig. 6d), indicating, most probably [18], that the system has crystallized.

## Synchrotron Analysis

*Phase transitions of 2(11)OBC.* The diffraction profiles corresponding to a cooling experiment similar to that used in the DSC experiments are shown in Figure 7. At high temperature, an amorphous halo is obtained in the WAXS channels, and no peak is observed in
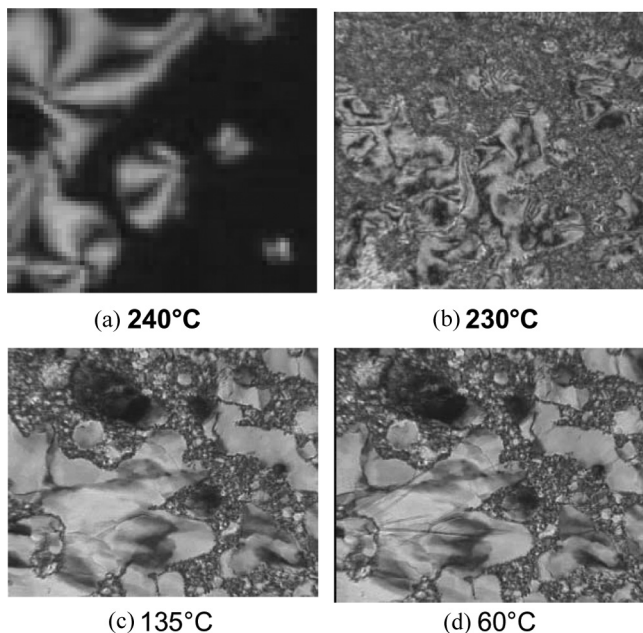
(a) **240°C**    (b) **230°C**

(c) 135°C    (d) 60°C

**FIGURE 5** Optical textures, at the indicated temperatures, of **(11)OBC** on cooling from the isotropic melt.

the MAXS region, as expected for the isotropic melt. Around 100°C, a sharp MAXS peak appears, centered at 2.870 nm, but the WAXS profile is rather similar to that of the isotropic state, indicating the formation of a low-ordered smectic mesophase, most probably of the type SmA. At *ca*. 89°C, the MAXS peak is shifted to 2.907 nm, and a considerable narrowing of the WAXS diffractogram is observed. These features are typical of a mesophase with disordered hexagonal packing within the smectic layers (probably a SmB mesophase).

On further lowering the temperature, at *ca*. 79°C, the WAXS diffractogram shows a very important modification, since three narrow diffractions peaks (at spacings of 0.454, 0.413 and 0.328 nm) are observed, while the MAXS peak changes only very slightly to a spacing of 2.915 nm. These characteristics, together with the textures obtained by optical microscopy, support the formation of a highly ordered smectic crystal with orthorhombic packing, as for a SE phase.

Finally, when the temperature reaches 47°C, the narrow MAXS peak disappears (although a broad and less intense peak seems to be present, centered at 2.70 nm) and the WAXS diffractogram presents
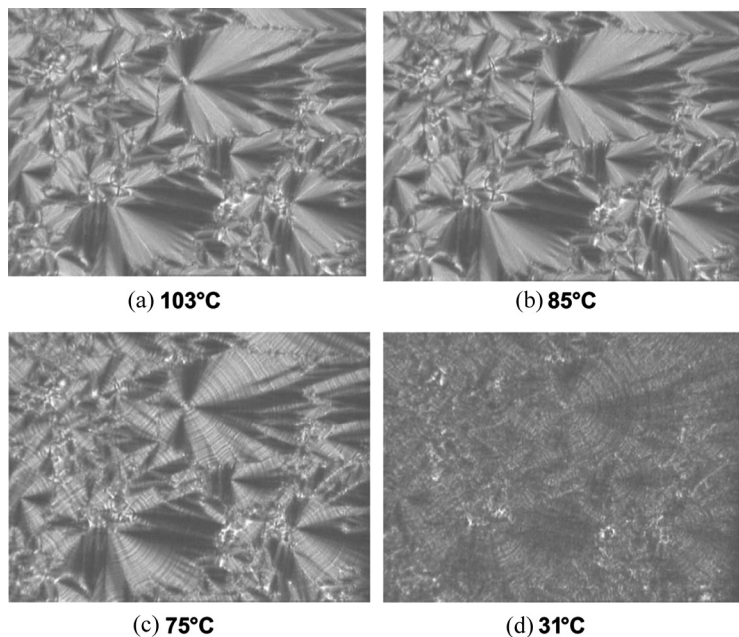
**FIGURE 6** Optical textures, at the indicated temperatures, of **2(11)OBC** on cooling from the isotropic melt.

several well defined diffraction peaks. A three-dimensional crystal structure seems to be formed below this temperature.

Therefore, considering all available data, DSC, optical textures and synchrotron results, the phase transitions sequence for **2(11)OBC** on cooling is the following: Isotropic → SmA (101°C) → SmB (88°C) → SE (79°C) → crystal phase (43°C).

*Phase transitions of (11)OBC.* The diffraction profiles corresponding to the first melting experiment of this sample are shown in Figure 8. At low temperatures, no peak is observed in the MAXS region, while diffraction peaks are detected in the WAXS diffractogram. These characteristics, together with the texture obtained by optical microscopy, support the presence of a three-dimensional crystal structure at low temperature.

On heating, when the temperature is about 116°C, a clearly defined MAXS peak appears, centered at 3.47 nm, and the WAXS diffractogram shows important changes. This is attributed to the formation, totally completed at 124°C, of a highly ordered smectic crystal, probably a SE mesophase. At *ca.* 172°C, within a temperature range
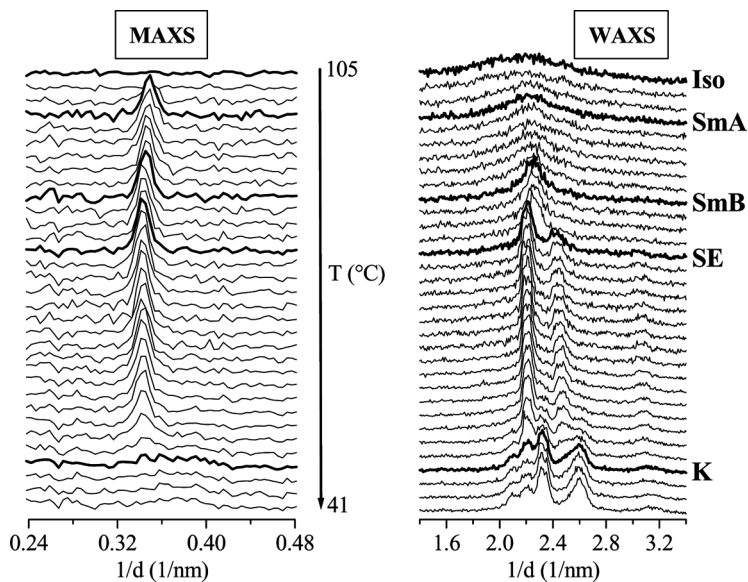
*D. López-Velázquez et al.*

**FIGURE 7** MAXS (left) and WAXS (right) profiles corresponding to the monomer **2(11)OBC** in a cooling experiment from the isotropic melt.
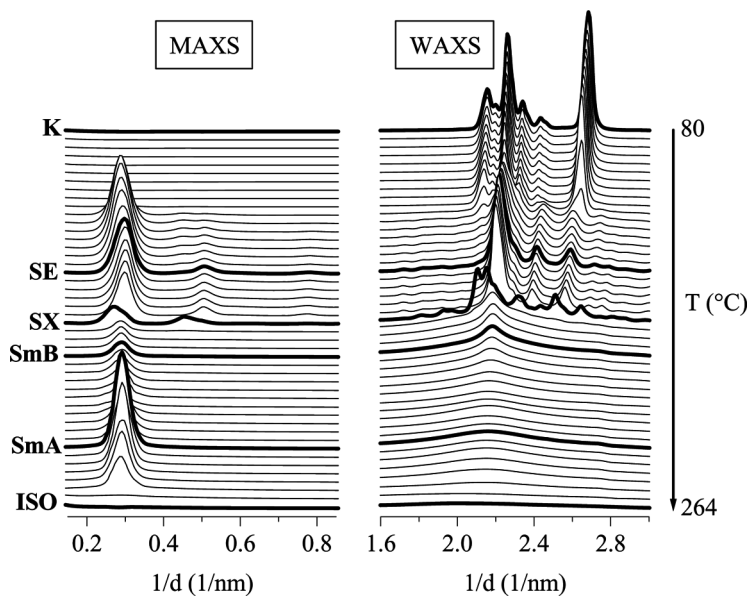


**FIGURE 8** MAXS (left) and WAXS (right) profiles for the biphenyl derivative **(11)OBC** in the first melting experiment.

corresponding to a single frame, a new structure is evident, which is assigned to an unknown SX smectic crystal. This phase immediately transforms into a new phase where the MAXS peaks decrease significantly in intensity, while the WAXS profile is reduced to a single, relatively broad halo, indicating the formation of a smectic mesophase of lower order. Since the WAXS halo is not very broad, a smectic mesophase of intermediate order seems to be present. These features are typical of a mesophase with disordered hexagonal packing within the smectic layers (probably a SmB mesophase). A close inspection of the DSC melting curve (Fig. 3) seems to indicate that the peak centered at 172.2°C is actually composed of two overlapped endotherms, corresponding to the formation of the SX and SmB phases. On further increasing of the temperature to *ca.* 188°C, the MAXS peak intensity increases again, while the WAXS halo is now considerably wider and amorphous-like. This is interpreted as the formation of a low-ordered SmA mesophase, related to the small endotherm observed in the DSC curve. Finally, above 256°C the isotropization of this mesophase is obtained.

On cooling from the isotropic melt, the phase sequence is practically the same (with an undercooling of *ca* 5–10°C) except for the fact that the two transitions from SmB to SX and from SX to SE are clearly resolved (see Fig. 3). Therefore, considering all the DSC, optical textures and synchrotron results, the phase transitions sequence (on cooling) for **(11)OBC** is: Isotropic → SmA (246°C) → SmB (192°C) → SX (162°C) → SE (148°C) → crystal phase (62°C).

On the other hand, considering that the length of the **(11)OBC** molecule, assuming an all-*trans* conformation for the alkyl chain, is calculated to be 2.58 nm, the MAXS spacing value of 3.47 nm supports the presence of dimeric species, formed through intermolecular hydrogen bonds between the carboxylic groups. MAXS and IR data are thus in agreement for **(11)OBC**. Intercalated and/or tilted structures may be involved in the solid state for this molecule.

On the contrary, the MAXS spacings observed for **2(11)OBC** (around 2.9 nm) are close to the extended chain length of this molecule.

## CONCLUSION

Both 4′-*n*-undecyloxybiphenyl-4-carboxylic acid, **(11)OBC**, and ethyl 4′-(*n*-undecyloxy)-biphenyl-4-carboxylate, **2(11)OBC**, were obtained in high yields and the latter compound has been characterized by single-crystal X-ray diffraction. Both biphenyl derivatives have high or relatively high clearing points and large liquid crystal phase ranges

with a rich polymesomorphism. However, **(11)OBC** exhibits significantly higher clearing point and larger mesophase ranges. These differences can be ascribed to the higher polarity of the acid group, which probably forms dimers by hydrogen bonds associations, giving a longer mesogenic structure. The large temperatures range of the smectic mesophases, on heating and cooling, supports the existence of **(11)OBC** as a dimerized carboxylic acid. Therefore, the thermal behavior of **(11)OBC** is determined mainly by the acid group, a fact consistent with all reported data. Considering all the DSC, optical textures and synchrotron results, the phase transitions sequences for **2(11)OBC** and **(11)OBC** were determined.

## REFERENCES

[1] Hirschmann, H. & Reiffenrath, V. (1998). In: *Handbook of Liquid Crystals*, Demus, D., Goodby, J., Gray, G. W., Spiess, H.-W., & Vill, V. (Eds.), Wiley-VCH: Weinheim, Germany, Vol. 2A, p. 199.

[2] Toyne, K. J. (1998). *Handbook of Liquid Crystals*, Demus, D., Goodby, J., Gray, G. W., Spiess, H.-W., & Vill, V. (Eds.), Wiley-VCH: Weinheim, Germany, Vol. 2A, p 47.

[3] Mcardle, C. B., Ed. (1989). *Side Chain Liquid Crystal Polymers*, Blackie: Glasgow, London, p. 357.

[4] Gray, G. W., Hartley, J. B., & Jones, B. (1955). *J. Chem. Soc.*, 1412.

[5] Isoo, K., Takayuki, H., Shoji, T., Masayashi, M., Chizu, S., & Takeshi, T. (1990). *Chem. Abstr.*, *115*, 18727V.

[6] (1996). *XSCAnS* (release 2.21) Users Manual, Siemens Analytical X-ray Instruments Inc.; Madison, WI.

[7] Sheldrick, G. M. (1997). *SHELX97*, Users Manual. University of Göttingen: Göttingen, Germany.

[8] Vogel, A. I., Tatchell, A. R., Furnis, B. S., & Hannaford A. J. (1996). *Vogel's Textbook of Practical Organic Chemistry*, 5th ed., Prentice Hall, p. 1552.

[9] Rajnikant Gupta, V. K., Dinesh Kumar, A., & Varghese, B. (2003). *Kristallografiya*, *48*, 321.

[10] Rajnikant Gupta, V. K., Gupta, R., Kumar, A., Bamezai, R. K., Sharma, N. K., & Varghese, B. (2000). *Kristallografiya*, *45*, 104.

[11] Rajnikant Gupta, V. K., Dinesh Kumar, A., & Varghese, B. (2002). *Mol. Cryst. Liq. Cryst. Sci. Technol.*, *A383*, 99.

[12] Hori, K., Kurosaki, M., Wu, H., & Itoh, K. (1996). *Acta Crystallogr.*, *52*, 1751.

[13] Davey, R. J., Gillon, A. L., Quayle, M. J., & Rashad, O. (2005). *Acta Crystallogr.*, *61*, 143.

[14] Lee, J. Y., Painter, P. C., & Coleman, M. M. (1988). *Macromolecules*, *21*, 954.

[15] Kato, T. & Fréchet J. M. J. (1989). *Macromolecules*, *22*, 3818.

[16] March, J. (1992). *Advanced Organic Chemistry: Reactions, Mechanism and Structure*, 4th ed., John Wiley & Sons, Inc., New York, 75.

[17] Demus, D. & Richter, L. (1980). *Textures of Liquid Crystals*, 2nd ed., VEB Deutscher Verlag für Grundstoffindustries: Leipzig.

[18] Bouligand, Y. (1998). *Handbook of Liquid Crystal*, Demus, D., Goodby, J., Gray, G. W., Spiess, H.-W. & Vill, V. (Eds.), Wiley-VCH: Weinheim, Germany, Vol. 1, 406.

[19] Chandrasekhar, S. (1992). *Liquid Crystals*, 2nd ed., Cambridge University Press: Cambridge.